The Canadian Mineralogist
Vol. 52, pp. 745-762 (2014)
DOI: 10.3749/canmin.1400043

SAAMITE, $Ba\square TiNbNa_3Ti(Si_2O_7)_2O_2(OH)_2(H_2O)_2$, A GROUP-III Ti-DISILICATE MINERAL FROM THE KHIBINY ALKALINE MASSIF, KOLA PENINSULA, RUSSIA: DESCRIPTION AND CRYSTAL STRUCTURE

FERNANDO CÁMARA[§]

Dipartimento di Scienze della Terra, Università degli Studi di Torino, via Valperga Caluso 35, 10125 Torino, Italy
Interdepartmental Centre for Crystallography, Via P. Giuria 5, I-10125, Torino, Italy and
Department of Geological Sciences, University of Manitoba, Winnipeg, Manitoba R3T 2N2, Canada

ELENA SOKOLOVA, YASSIR A. ABDU, AND FRANK C. HAWTHORNE

Department of Geological Sciences, University of Manitoba, Winnipeg, Manitoba R3T 2N2, Canada

ABSTRACT

Saamite, $Ba\square TiNbNa_3Ti(Si_2O_7)_2O_2(OH)_2(H_2O)_2$, is a Group-III TS-block mineral from the Kirovskii mine, Mount Kukisvumchorr, Khibiny alkaline massif, Kola Peninsula, Russia. The mineral occurs as transparent platy crystals 2–10 μm thick and up to 180 μm across. It is colorless to very pale tan, with a white streak and a vitreous luster. The mineral formed in a pegmatite as a result of hydrothermal activity. Associated minerals are natrolite, barytolamprophyllite, kazanskyite, nechelyustovite, hydroxylapatite, belovite-(La), belovite-(Ce), gaidonnayite, nenadkevichite, epididymite, apophyllite-(KF), and sphalerite. Saamite has perfect cleavage on {001}, uneven fracture and a Mohs hardness *ca.* 3. Its calculated density is 3.243 g/cm^3. Saamite is biaxial positive with α 1.760, β 1.770, γ 1.795 (λ 589 nm), $2V_{meas.}$ = 69(2)°, $2V_{calc.}$ = 65°, with medium dispersion, $r > v$. It is nonpleochroic. Saamite is triclinic, space group $P\bar{1}$, a 5.437(2), b 7.141(3), c 21.69(1) Å, α 92.97(1), β 96.07(1), γ 90.01(1)°, V 836.3(11) Å^3. The strongest lines in the X-ray powder-diffraction pattern [d(Å)(I)(hkl)] are: 21.539(100)(001), 2.790(15)(122), 2.692(14)(008), 3.077(13)(007), 7.180(11)(003), 2.865(11)(1$\bar{2}$2), 1.785(9)(1$\bar{1}$4), 2.887(9)($\bar{1}$22, 0$\bar{1}$7, 115), and 1.785(9)(0$\bar{4}$1, 1$\bar{3}$7, 040, $\bar{2}\bar{2}$8, 230, 23$\bar{1}$). Chemical analysis by electron microprobe gave Nb_2O_5 12.24, TiO_2 20.37, SiO_2 29.07, Al_2O_3 0.08, FeO 0.32, MnO 5.87, MgO 0.04, BaO 11.31, SrO 2.51, CaO 1.76, K_2O 0.77, Na_2O 8.39, H_2O 5.77, F 1.71, O = F −0.72, sum 99.49 wt.%; H_2O was determined from structure refinement and its presence was confirmed by IR spectroscopy. The empirical formula based on 20 (O + F) atoms *pfu* is $(Ba_{0.61}Sr_{0.20}K_{0.13}\square_{0.06})_{\Sigma1}(\square_{0.74}Ca_{0.26})_{\Sigma1}(Na_{2.22}Mn_{0.55}Fe^{2+}_{0.04}\square_{0.19})_{\Sigma3}(Ti_{2.09}Nb_{0.76}Mn_{0.13}Mg_{0.01}Al_{0.01})_{\Sigma3}Si_{3.97}O_{19.26}H_{5.26}F_{0.74}$, Z = 2. The simplified formula is as follows: Ba(□,Ca)Ti(Nb,Ti)(Na,Mn)$_3$(Ti,Nb)$(Si_2O_7)_2O_2(OH,F)_2(H_2O)_2$. The IR spectrum of saamite contains the following bands: ~1605, 1645, ~1747 and ~3420 cm^{-1}. The crystal structure was solved by direct methods and refined to an R_1 index of 9.92%. In the crystal structure of saamite, the main structural unit is the TS block, which consists of HOH sheets (H-heteropolyhedral, O-octahedral). The TS block exhibits linkage and stereochemistry typical for Group III [Ti (+ Nb + Mg) = 3 *apfu*] of TS-block minerals. The O sheet is composed of Na- and Ti-dominant octahedra and has ideal composition Na_3Ti *apfu*. The TS block has two different H sheets where Si_2O_7 groups link to [5]-coordinated Ti and [6]-coordinated Nb polyhedra, respectively. There are two peripheral sites, [10]-coordinated $A^P(1)$ and [8]-coordinated $A^P(2)$, occupied mainly by Ba (less Sr and K) at 94% and Ca at 26%, respectively. In the crystal structure of saamite, adjacent TS blocks connect in two different ways: (1) via hydrogen bonds between H_2O–H_2O groups and H_2O–O atoms of adjacent TS blocks; (2) via a layer of Ba atoms that constitute the **I** block. The TS block, **I** block and types of self-linkage of TS blocks are topologically identical to those in the nechelyustovite structure. The mineral is named after the Saami (Саами in Cyrillic) indigenous people who inhabit parts of the Kola Peninsula of Russia, far northern Norway, Sweden, and Finland.

Keywords: saamite, new mineral, Khibiny alkaline massif, Kola Peninsula, Russia, crystal structure, Group III, Ti-disilicate, TS block.

§ *Corresponding author e-mail address*: fernando.camaraartigas@unito.it

Introduction

Saamite, ideally $Ba\square TiNbNa_3Ti(Si_2O_7)_2O_2(OH)_2(H_2O)_2$, is a new representative of the Ti-disilicate minerals with the TS (titanium silicate) block (Sokolova 2006). In the crystal structure of saamite, the TS block has the stereochemistry and topology of Group III where Ti (+ Nb + Mg) = 3 *apfu* (atoms per formula unit). In Group III, the TS block exhibits linkage 1, where the Si_2O_7 groups of two H sheets link to the *trans* edges of the Ti octahedron of the O sheet (Sokolova 2006). Other Group-III minerals are as follows: lamprophyllite, nabalamprophyllite, barytolamprophyllite, lileyite, epistolite, vuonnemite, innelite, bornemanite, kazanskyite, and nechelyustovite (Table 1). The crystal structure of saamite is a new structure type and does not have any analogues.

The name is after the Saami (also spelled Sámi or Sami, Саами in Cyrillic) indigenous people who inhabit parts of the Kola Peninsula of Russia, far northern Norway, Sweden, and Finland. The name saamite was previously used for a strontium- and REE-bearing fluorapatite from the Kola peninsula (Volkova & Melentiev 1939), although it was not a recognized mineral name. The new mineral species and its name have been approved by the Commission on New Minerals, Nomenclature and Classification of the International Mineralogical Association (IMA 2013-083). The holotype specimen of saamite is deposited at the Fersman Mineralogical Museum, Russian Academy of Sciences, Leninskii Pr. 18/2, 117071 Moscow, Russia, registration numbers 4432/1 and 4432/2.

Occurrence and Associated Minerals

Saamite was discovered in a sample of nechelyustovite (Cámara & Sokolova 2009) and kazanskyite (Cámara *et al.* 2012) from the underground Kirovskii mine (+252 m level), Mount Kukisvumchorr, Khibiny alkaline massif, Kola Peninsula, Russia; this sample is in the mineral collection of Adriana and Renato Pagano, Milan, Italy (Collezione Mineralogica, sample 10161c). Here we give a description of the mineral association of saamite following Nèmeth *et al.* (2009), who described the mineral association for nechelyustovite. Nechelyustovite was found in one hydrothermally altered pegmatite body emplaced in nepheline syenites near their contact with ijolite-urtites. The pegmatite is a branching vein 0.1–0.5 m wide with a symmetrical zoned structure: a natrolite core, a microcline zone, and a marginal aegirine-dominated external zone with subordinate amounts of microcline, nepheline, lamprophyllite, and eudialyte. Nechelyustovite (and saamite and kazanskyite) is confined to the natrolite core where it forms rosettes up to 5 cm in diameter composed of extremely fine (0.01–0.1 mm) bounded flakes and lamellae, embedded in a matrix of natrolite or carbonate-rich hydroxylapatite. Other associated minerals are barytolamprophyllite, belovite-(La), belovite-(Ce), gaidonnayite, nenadkevichite, epididymite, apophyllite-(KF), and sphalerite.

Physical and Optical Properties

The main properties of saamite are presented in Table 2, where they are compared to those of the Group-III minerals barytolamprophyllite, epistolite, kazanskyite, and nechelyustovite. The mineral forms transparent platy crystals 2–10 μm thick and up to 180 μm across (Fig. 1). Saamite is colorless to very, very pale tan, with a white streak and a vitreous luster. Saamite crystals have a perfect {001} cleavage, uneven fracture, and Mohs hardness of *ca.* 3, and are non-fluorescent under 240–400 nm ultraviolet radiation. The density of the mineral could not be measured owing to paucity of material. Its calculated density (using the empirical formula) is 3.243 g/cm^3. Saamite is biaxial positive with α 1.760, β 1.770, γ 1.795 (λ 589 nm), all ±0.005, $2V_{meas.}$ = 69(2)°, $2V_{calc.}$ = 65°, with medium dispersion, $r > v$. It is nonpleochroic. Optical orientation is given in Table 3. A Gladstone-Dale calculation (Mandarino 1979,1981) gives a compatibility index of 0.025, which is rated as excellent.

Fourier-transform infra-red (FTIR) spectroscopy

A transmission FTIR spectrum was collected on a crystal fragment using a Bruker Hyperion 2000 IR microscope equipped with a liquid-nitrogen-cooled MCT detector. The spectrum over the range 4000−650 cm^{-1} was obtained by averaging 100 scans with a resolution of 4 cm^{-1}. In the principal O–H stretching region (4000–3000 cm^{-1}), the FTIR spectrum (Fig. 2) shows a broad band centered at ~3420 cm^{-1}, with two side bands at ~3540 cm^{-1} and 3260 cm^{-1}. The 3540 cm^{-1} band may be assigned to O–H stretches of the OH group, and the 3420 and 3260 cm^{-1} bands to O–H stretches of H_2O in the saamite structure. The H_2O bends occur at ~1645 and 1605 cm^{-1} (a shoulder). The peak at ~1747 cm^{-1} is probably a combination band.

Chemical Composition

For the chemical analysis, we used a platy crystal of saamite with dimensions 0.01 × 0.10 × 0.18 mm. The chemical composition of saamite was determined with a Cameca SX-100 electron-microprobe in wavelength-dispersion mode with an accelerating voltage of 15 kV, a specimen current of 5 nA, a beam size of 20 μm, and count times on peak and background of 20 and 10 s, respectively. The following standards were used: $Ba_2NaNb_5O_{15}$ (Ba,Nb), $SrTiO_3$ (Sr), titanite (Ti,Si), diopside (Ca), andalusite (Al), fayalite (Fe), spessartine (Mn), forsterite (Mg), orthoclase (K), albite (Na), and F-bearing riebeckite (F). Tantalum, Zr, Zn, P, and Cs were sought but not detected. Data were reduced using the PAP procedure of Pouchou &

TABLE 1. IDEAL STRUCTURAL FORMULAE* AND UNIT-CELL PARAMETERS FOR GROUP-III MINERALS WITH THE TS-BLOCK

Mineral Structure type ***	Ideal structural formula									*a* (Å) α (°)	*b* (Å) β (°)	*c* (Å) γ (°)	Sp. gr.	*Z*	Ref.
	A_2^P	B_2^P	$\mathbf{M_2^H}$	$\mathbf{M_4^O}$		$\mathbf{(Si_2O_7)_2}$		$\mathbf{X_4^O}$							
Basic structures															
lamprophyllite-2*M* B1(GIII)	(SrNa)		$\mathbf{^{[5]}Ti_2}$	$\mathbf{Na_3}$	**Ti**	$\mathbf{(Si_2O_7)_2}$		$\mathbf{O_2(OH)_2}$		19.215 90	7.061 96.797	5.3719 90	*C*2/*m*	2	(1)
lamprophyllite-2*O* B1(GIII)	(SrNa)		$\mathbf{^{[5]}Ti_2}$	$\mathbf{Na_3}$	**Ti**	$\mathbf{(Si_2O_7)_2}$		$\mathbf{O_2(OH)_2}$		19.128 90	7.0799 90	5.3824 90	*Pnmn*	2	(1)
nabalamprophyllite-2*M* B1(GIII)	BaNa		$\mathbf{^{[5]}Ti_2}$	$\mathbf{Na_3}$	**Ti**	$\mathbf{(Si_2O_7)_2}$		$\mathbf{O_2(OH)_2}$		19.741 90	7.105 96.67	5.408 90	*P*2/*m*	2	(2)
nabalamprophyllite-2*O* B1(GIII)	(BaNa)		$\mathbf{^{[5]}Ti_2}$	$\mathbf{Na_3}$	**Ti**	$\mathbf{(Si_2O_7)_2}$		$\mathbf{O_2(OH)_2}$		19.564 90	7.1173 90	5.414 90	*Pnmn*	2	(3)
barytolamprophyllite B1(GIII)	(BaK)		$\mathbf{^{[5]}Ti_2}$	$\mathbf{Na_3}$	**Ti**	$\mathbf{(Si_2O_7)_2}$		$\mathbf{O_2(OH)_2}$		19.8971 90	7.1165 96.676	5.4108 90	*C*2/*m*	2	(4)
lileyite B1(GIII)	Ba_2		$\mathbf{^{[5]}Ti_2}$	$\mathbf{Na_2M^{2+}}$	$\mathbf{Mg_2}$	$\mathbf{(Si_2O_7)_2}$		$\mathbf{O_2F_2}$		19.905 90	7.098 96.349	5.405 90	*C*2/*m*	2	(5)
innelite-1*T* B2(GIII)	Ba_2	Ba_2	$\mathbf{^{[5]}Ti_2}$	$\mathbf{Na_2M^{2+}}$	**Ti**	$\mathbf{(Si_2O_7)_2}$	$[(SO_4)(PO_4)]$	$\mathbf{O_2[O(OH)]}$		5.4234 98.442	7.131 94.579	14.785 90.009	$P\bar{1}$	1	(6)
innelite-2*M* B2(GIII)	Ba_2	Ba_2	$\mathbf{^{[5]}Ti_2}$	$\mathbf{Na_2M^{2+}}$	**Ti**	$\mathbf{(Si_2O_7)_2}$	$[(SO_4)(PO_4)]$	$\mathbf{O_2[O(OH)]}$		5.4206 90	7.125 94.698	29.314 90	*P*2/*c*	2	(6)
epistolite B3(GIII)	(Na□)		$\mathbf{^{[6]}Nb_2}$	$\mathbf{Na_3}$	**Ti**	$\mathbf{(Si_2O_7)_2}$		$\mathbf{O_2(OH)_2}$	$(H_2O)_4$	5.460 103.63	7.170 96.01	12.041 89.98	$P\bar{1}$	1	(7)
vuonnemite B4(GIII)	Na_6	Na_2	$\mathbf{^{[6]}Nb_2}$	$\mathbf{Na_3}$	**Ti**	$\mathbf{(Si_2O_7)_2}$	$(PO_4)_2$	$\mathbf{O_2(OF)}$		5.4984 92.60	7.161 95.30	14.450 90.60	$P\bar{1}$	1	(8)
delindeite related****		Ba_2	$\mathbf{^{[6]}Ti_2}$	$\mathbf{Na_2(H_2O)}$	**Ti**	$\mathbf{(Si_2O_7)_2}$		$\mathbf{(OH)_2(H_2O)□}$	O_2	10.6452 90	13.713 93.804	21.600 90	*C*2/*c*	8	(9)
Derivative structures															
saamite D4(GIII)	Ba□		$\mathbf{^{[5]}Ti^{[6]}Nb}$	$\mathbf{Na_3}$	**Ti**	$\mathbf{(Si_2O_7)_2}$		$\mathbf{O_2(OH)_2}$	$(H_2O)_2$	5.437 92.97	7.141 96.01	21.69 90.01	$P\bar{1}$	2	(10)
bornemanite D1(GIII)	Na_3	BaNa	$\mathbf{^{[5]}Ti^{[6]}Nb}$	$\mathbf{Na_3}$	**Ti**	$\mathbf{(Si_2O_7)_2}$	(PO_4)	$\mathbf{O_3F}$		5.4587 96.790	7.1421 96.927	24.528 90.326	$P\bar{1}$	2	(11)
kazanskyite D2(GIII)	Ba□		$\mathbf{^{[5]}Ti^{[6]}Nb}$	$\mathbf{Na_3}$	**Ti**	$\mathbf{(Si_2O_7)_2}$		$\mathbf{O_2(OH)_2}$	$(H_2O)_4$	5.4260 98.172	7.135 90.916	25.514 89.964	$P\bar{1}$	2	(12)
nechelyustovite** D3(GIII)	(Na□)Ba_4□$_2$		$\mathbf{^{[5]}Ti_4^{[6]}Nb_4}$	$\mathbf{(Na_{11}□)}$	$\mathbf{Ti_4}$	$\mathbf{(Si_2O_7)_8}$		$\mathbf{O_8(OH)_8}$	$(H_2O)_{12}$	5.4468 92.759	7.157 92.136	47.259 89.978	$P\bar{1}$	1	(13)

* The formula is given per $(Si_2O_7)_2$; for lamprophyllite, nabalamprophyllite, and barytolamprophyllite, formulae are from Sokolova (2006); for bornemanite and nechelyusovite, from Sokolova & Cámara (2013). The invariant core of the TS-block, $\mathbf{M_2^H M_4^O (Si_2O_7)_2 X_4^O}$, is shown in bold: M^H = cations of the H sheet; M^O = cations of the O sheet; X_4^O = anions shared between O and H sheets and not bonded to Si; M^{2+} = Fe^{2+},Ca,Mn (lileyite); M^{2+} = Mn,Fe^{2+},Mg,Ca (innelite);
** formula is given per $(Si_2O_7)_8$;
*** structure types for basic (B) and derivative (D) structures are in accord with Sokolova & Cámara (2013);
**** due to the Na-H_2O disorder in the O sheet, TS block in delindeite exhibits stereochemistry of Group I.

References (the most recent reference on the structure): (1) Krivovichev *et al.* (2003); (2) Rastsvetaeva and Chukanov (1999); (3) Sokolova and Hawthorne (2008); (4) Sokolova and Cámara (2008); (5) Chukanov *et al.* (2012); (6) Sokolova *et al.* (2011); (7) Sokolova and Hawthorne (2004); (8) Ercit *et al.* (1998); (9) Sokolova and Cámara (2007); (10) this work; (11) Cámara and Sokolova (2007); (12) Cámara *et al.* (2012); (13) Cámara and Sokolova (2009).

TABLE 2. COMPARATIVE TABLE FOR SAAMITE, BARYTOLAMPROPHYLLITE, KAZANSKYITE, AND NECHELYUSTOVITE

Formula	saamite $Ba\square Na_3Ti_2Nb$ $(Si_2O_7)_2O_2(OH)_2(H_2O)_2$	barytolamprophyllite* $(BaK)Na_3Ti_3$ $(Si_2O_7)_2O_2(OH)_2$	kazanskyite $Ba\square Na_3Ti_2Nb$ $(Si_2O_7)_2O_2(OH)_2(H_2O)_4$	nechelyustovite* $Na_4Ba_2Mn_{1.5}\square_{2.5}Ti_5Nb$ $(Si_2O_7)_4O_4(OH)_3F(H_2O)_6$	
Reference	(1)	(2, 3, 4)	(5)	(6)	(7)
system	triclinic	monoclinic	triclinic	monoclinic	triclinic
space group	$P\bar{1}$	$C2/m$	$P\bar{1}$	$A2/m$	$P\bar{1}$
a (Å)	5.437(2)	10.8971	5.4260	5.38	5.447
b	7.141(3)	7.1165	7.135	7.04	7.157
c	21.69(1)	5.4108	25.514	48.10	47.259
α (°)	92.97(1)	90	98.172	90	95.759
β	96.07(1)	96.676	90.916	91.1	92.136
γ	90.01(1)	90	89.964	90	89.978
V (Å^3)	836.3(11)	760.96	977.61	1821	1831.7
Z	2	2	2	2	2
$D_{meas.}$ (g/cm^3)		3.543		3.32–3.42	
$D_{calc.}$ (g/cm^3)	3.243	3.521	2.927	3.20	3.041
Strongest lines in the powder pattern d_{meas} (I)	21.539(100), 7.180(11), 2.887(9), 2.865(11), 2.790(15), 2.692(14)	2.801(100), 2.153(90), 1.482(90), 1.601(80), 3.45(70), 1.790(70)	2.813(100), 2.149(82), 3.938(70), 4.288(44), 2.128(44), 3.127(39)	24.06(100), 7.05(9), 5.95(97), 3.95(6), 2.828(16), 2.712(19)	
Optical character	biaxial (+)	biaxial (+)	biaxial (+)	biaxial (+)	
α	1.760(5)	1.747	1.695	1.700	
β	1.770(5)	1.750	1.703	1.710	
γ	1.795(5)	1.773	1.733	1.734	
$2V_{meas.}$ (°)	69(2)	39.67	64.8		
$2V_{calc.}$ (°)	65.4		55.4	66.0	
Color	colorless to very pale tan	dark brown	colorless to very very pale tan	creamy with grayish, bluish or yellowish shades	

*barytolamprophyllite: formula, unit-cell parameters, space group and $D_{calc.}$ (4); powder pattern (2, p.65); $D_{meas.}$and optics (3); nechelyustovite: formula (7).
Reference: (1) this work; (2) Anthony *et al*. (1995); (3) Dudkin (1959); (4) Sokolova & Cámara (2008); (5) Cámara *et al*. (2012); (6) Nèmeth *et al.* (2009); (7) Cámara & Sokolova (2009).

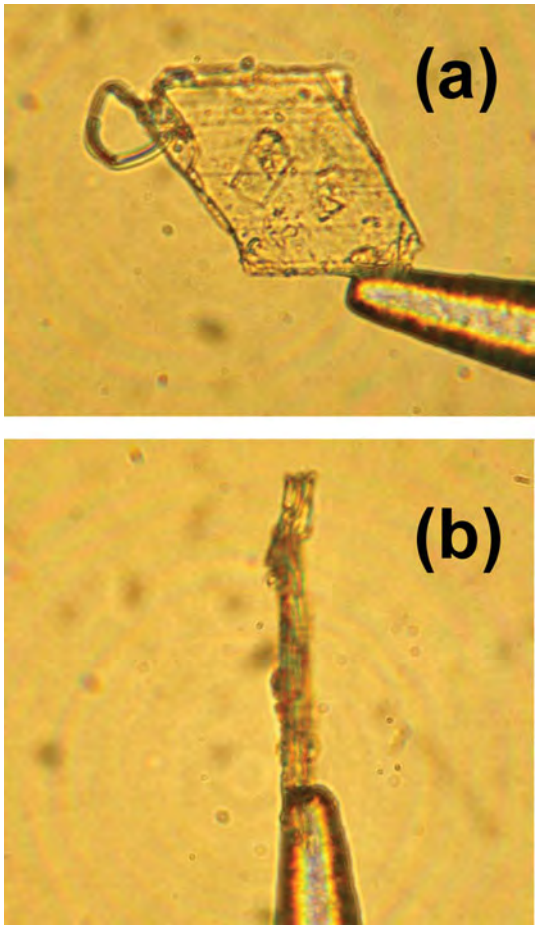

FIG. 1. The crystal of saamite used for measuring optics (~0.015 × 0.125 × 0.150 mm) on a glass fiber in oil. Note the platy nature (a) and irregular surface of the crystal (b).

TABLE 3. OPTICAL ORIENTATION (°) FOR SAAMITE

	a	b	c
X	85.0	94.8	11.1
Y	60.1	30.0	93.9
Z	149.6	60.5	79.6

Pichoir (1985). Under an electron beam, saamite is extremely unstable. For Na_2O, 8.39 wt.% was achieved only for the first point and attempts to analyze this grain again resulted in much lower values for Na_2O, ~5.5–7.5 instead of > 8 wt.% from the first point. We conclude that saamite grains are very heterogeneous and, under the electron beam, saamite loses Na. To calculate the empirical formula of saamite in accordance with the structure results, we used the Na_2O value from point 1. We did not have material sufficient for direct determination of H_2O, but the presence of H_2O was confirmed by FTIR spectroscopy (see above). H_2O was calculated from the results of the crystal structure analysis on the basis of OH = 1.26 *pfu* and H_2O = 2 *pfu* (per formula unit). The chemical composition of saamite is given in Table 4. The empirical formula based on 20 (O + F) atoms *pfu* is $(Ba_{0.61}Sr_{0.20}K_{0.13}\square_{0.06})_{\Sigma1}(\square_{0.74}Ca_{0.26})_{\Sigma1}(Na_{2.22}Mn_{0.55}Fe^{2+}_{0.04}\square_{0.19})_{\Sigma3}Si_{3.97}O_{19.26}H_{5.26}F_{0.74}$, Z = 2. The structural formula of the form $A^P_2M^H_2M^O_4(Si_2O_7)_2X^O_4X^P_MX^P_A$ is $(Ba_{0.61}Sr_{0.20}K_{0.13}\square_{0.06})_{\Sigma1}(\square_{0.74}Ca_{0.26})_{\Sigma1}(Ti_{0.87}Nb_{0.12}Al_{0.01})_{\Sigma1}(Nb_{0.55}Ti_{0.45})_{\Sigma1}(Na_{2.22}Mn_{0.55}Fe^{2+}_{0.04}\square_{0.19})_{\Sigma3}(Ti_{0.77}Mn_{0.13}Nb_{0.09}Mg_{0.01})_{\Sigma1}(Si_4O_7)_2O_2[(OH)_{1.26}F_{0.74}]_{\Sigma2}(H_2O)(H_2O)$. Simplified and ideal formulae are as follows: $Ba(\square,Ca)Ti(Nb,Ti)(Na,Mn)_3(Ti,Nb)(Si_2O_7)_2O_2\ (OH,F)_2(H_2O)_2$ and $Ba\square TiNbNa_3Ti(Si_2O_7)_2O_2(OH)_2(H_2O)_2$.

CRYSTAL STRUCTURE

X-ray data collection and structure refinement

All crystals of saamite that we were able to find were twinned. X-ray diffraction data for the crystal of saamite (0.080 × 0.020 × 0.007 mm) were collected with a Bruker APEX II Ultra three-circle diffractometer with a rotating-anode generator (MoKα), multilayer optics and an APEX-II 4K CCD detector. The intensities of 21994 reflections with $-7 \le h \le 7$, $-9 \le k \le 9$, $-12 \le l \le 28$ were collected to 55° 2θ using 0.3° frame and an integration time of 20 s. The refined unit-cell parameters were obtained from 8719 reflections with $I > 10\sigma I$ (Tables 2, 6). The crystal was found to be a non-merohedral twin with a two-fold rotation on [001] and showed residual disorder caused by rotation along [100], probably due to some degree of crystal bending. CELL NOW (Sheldrick 2004) was used to obtain an HKLF5 file, and an empirical absorption correction (TWINABS, Sheldrick 2008) was applied. The crystal structure of saamite was solved with the Bruker SHELXTL Version 5.1 system of programs (Sheldrick 2008) in space group $P\bar{1}$ by direct methods and refined to R_1 = 9.92% based on 3444 unique reflections with $F > 4\sigma(F)$, the twin ratio being 0.970(3):0.030(3). Site-scattering values were refined for the $M^H(1,2)$ and $M^O(1)$ sites with the scattering curve of Nb and Ti, respectively, $M^O(2)$ site (scattering curve of Na), $M^O(3,4)$ sites (scattering curve of Mn), and $A^P(1)$ and $A^P(2)$ sites with the scattering curves of Ba and Ca, respectively. After refinement of the site occupancy for the $A^P(2)$ site, it was adjusted in accordance with the chemical analysis and mean bond length, and fixed. For saamite, we observed disorder at the $[A^P(2) + X^P_A]$ and *W* sites, partly occupied by [Ca and H_2O] and H_2O, respectively, and separated by short distances $A^P(2)$–W = 0.96(19) Å and X^P_A–W = 1.67(19) Å.

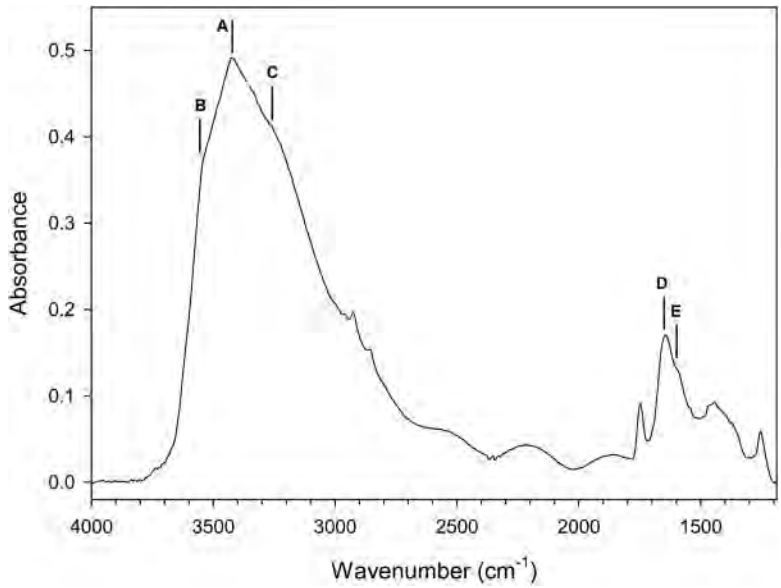

FIG. 2. FTIR spectrum of saamite, excluding the fingerprint region due to saturation. Bands A–C correspond to the principal O–H stretching vibrations A ~3420 cm^{-1}, with two side bands at B ~3540 cm^{-1} and C ~3260 cm^{-1}. Bands D at ~1645 cm^{-1} and E at 1605 cm^{-1} (a shoulder) are the H_2O bends. The peak at ~1747 cm^{-1} is probably a combination band.

TABLE 4. CHEMICAL COMPOSITION AND UNIT FORMULA* FOR SAAMITE

Oxide	wt.%	range	SD	Formula unit	*apfu*
Nb_2O_5	12.24	10.6–13.8	0.81	Si	3.97
TiO_2	20.37	18.04–20.37	0.83		
SiO_2	29.07	28.22–30.28	0.72	Na	2.22
Al_2O_3	0.08	0.06–0.13	0.02	Mn	0.55
FeO	0.32	0.15–0.32	0.05	Fe^{2+}	0.04
MnO	5.87	5.37–6.38	0.27	$\Sigma 3M^O$	2.81
MgO	0.04	0.01–0.07	0.02		
BaO	11.31	2.26–3.09	0.28	Ti	2.09
SrO	2.51	9.71–12.07	0.61	Nb	0.76
CaO	1.76	1.62–1.95	0.08	Mn	0.13
K_2O	0.77	0.68–0.90	0.06	Mg	0.01
Na_2O**	8.39	5.52–8.39	0.98	Al	0.01
H_2O***	5.77			$\Sigma(2M^H+M^O)$	3.00
F	1.71	1.31–1.89	0.19		
$O=F_2$	−0.72			Ba	0.61
Total	99.49			Ca	0.26
				Sr	0.20
				K	0.13
				$\Sigma[A^P(1)+ A^P(2)]$	1.20
				F	0.74
				OH	1.26
				H_2O	2.00

*calculated on anion basis: O + F = 20 *apfu*;
**the value at the first point (see text);
***calculated from structure solution and refinement: OH = 1.26 *pfu*, H_2O = 2 *pfu*.

Site occupancies for the X^P_A and W sites were refined with U_{iso} fixed at 0.05 Å^2 (analogous to U_{eq} of the X^P_M site fully occupied by H_2O), and then fixed. At the last stages of the refinement, six peaks with magnitudes from 1.32 to 2.83 e/Å^3 were found in the difference-Fourier map, most of the these peaks occurring in the vicinity of the A^P(1,2) sites. Occupancies for peaks 1 and 2–6 were refined with the scattering curve of Ti and Ba with U_{iso} fixed at 0.02 Å^2 (except for 1). Refined occupancies of these subsidiary peaks vary from 2 to 9%. Scattering curves for neutral atoms were taken from the International Tables for Crystallography (Wilson 1992). Powder data were obtained by collapsing single-crystal X-ray diffraction data into two dimensions (Table 5) using XPREP v. 2005/1. Details of data collection and structure refinement are given in Table 6, final atom parameters are given in Table 7, selected interatomic distances in Table 8, refined site-scattering values and assigned populations for selected cation sites are given in Table 9, and bond-valence values in Table 10. A list of observed and calculated structure factors and a CIF file may be obtained from The Depository of Unpublished Data on the MAC website [document Saamite CM52-4_10.3749/canmin.1400043].

TABLE 5. X-RAY POWDER DIFFRACTION DATA FOR SAAMITE

$I_{obs.}$	d_{obs} (Å)	h	k	l	$I_{obs.}$	$d_{obs.}$ (Å)	h	k	l
100	21.539	0	0	1	6	2.162	$\bar{2}$	$\bar{2}$	1
11	7.180	0	0	3		2.161	$\bar{2}$	2	1
6	4.320	$\bar{1}$	1	0		2.160	$\bar{2}$	2	0
	4.310	$\bar{1}$	$\bar{1}$	1		2.158	$\bar{1}$	2	7
	4.308	0	0	5		2.155	$\bar{2}$	$\bar{2}$	2
	4.296	1	1	0		2.154	0	0	10
6	3.890	$\bar{1}$	$\bar{1}$	3	7	2.148	2	2	0
7	3.618	1	$\bar{1}$	3		2.147	$\bar{2}$	0	7
	3.605	0	1	5		2.142	$\bar{1}$	1	9
5	3.566	0	2	0		2.141	1	3	1
	3.565	$\bar{1}$	$\bar{1}$	4	7	2.142	$\bar{1}$	1	9
	3.558	$\bar{1}$	0	5		2.141	1	3	1
5	3.512	1	1	3		2.140	$\bar{2}$	2	2
7	3.141	0	1	6		2.139	1	$\bar{3}$	2
	3.135	$\bar{1}$	1	5		2.138	2	$\bar{2}$	1
	3.129	0	2	3		2.135	$\bar{1}$	3	2
13	3.077	0	0	7		2.134	0	3	4
5	2.972	1	$\bar{1}$	5	8	2.039	2	$\bar{2}$	3
	2.969	1	2	0		2.038	$\bar{2}$	1	7
	2.962	$\bar{1}$	2	1		2.037	0	3	5
9	2.887	$\bar{1}$	2	2		2.036	1	2	7
	2.880	0	$\bar{1}$	7		2.033	0	1	10
	2.880	1	1	5		2.031	0	$\bar{3}$	6
11	2.865	1	$\bar{2}$	2	9	1.785	0	$\bar{4}$	1
15	2.790	1	2	2		1.783	1	$\bar{3}$	7
7	2.741	1	$\bar{2}$	3		1.783	0	4	0
14	2.692	0	0	8		1.783	$\bar{2}$	$\bar{2}$	8
	2.692	1	$\bar{1}$	6		1.780	2	3	0
	2.690	$\bar{2}$	0	2		1.779	2	$\bar{3}$	1
7	2.627	$\bar{1}$	2	4	6	1.616	$\bar{3}$	2	1
	2.623	$\bar{2}$	0	3		1.615	$\bar{3}$	$\bar{2}$	2
	2.572	$\bar{1}$	1	7		1.614	$\bar{3}$	$\bar{2}$	1
	2.570	$\bar{1}$	$\bar{2}$	5		1.612	$\bar{3}$	2	0
	2.563	0	$\bar{1}$	8		1.611	$\bar{3}$	2	2
	2.560	1	0	7					

Site-population assignment

We divide the cation sites into 3 groups: M^O sites of the O sheet, M^H and *Si* atoms of the H sheet, and the peripheral A^P sites; site labeling is in accordance with Sokolova (2006).

We assign cations to the Ti(+ Nb)-dominant M^O and M^H sites based on our knowledge from previous work on Ti-disilicate minerals: Ti- and Nb-dominant sites are always fully occupied and the O sheet can have a significant Mn content [as in nechelyustovite (Cámara & Sokolova 2009)]. Table 4 shows that the

TABLE 6. MISCELLANEOUS REFINEMENT DATA FOR SAAMITE

a (Å)	5.437(2)
b	7.141(3)
c	21.69(1)
α (°)	92.97(1)
β	96.07(1)
γ	90.01(1)
V (Å^3)	836.3(11)
Space group	$P\bar{1}$
Z	2
Absorption coefficient (mm^{-1})	4.62
F(000)	781.8
$D_{calc.}$ (g/cm^3)	3.243
Crystal size (mm)	0.080 × 0.020 × 0.007
Radiation/monochromator	MoKα/graphite
2θ-range used for structure refinement (°)	2.67–54.99
R(int) (%)	6.42
Reflections collected	21994
Independent reflections	3816
$F_o > 4\sigma F$	3444
Refinement method	Full-matrix least squares on F^2, fixed weights proportional to $1/\sigma Fo^2$
No. of refined parameters	306
Final $R_{(obs)}$ (%) [$F_o > 4\sigma F$]	9.96
R_1	10.79
wR_2	23.05
Highest peak, deepest hole (e Å^{-3})	+1.93 −3.12
Goodness of fit on F^2	1.264

TABLE 7. ATOM COORDINATES AND EQUIVALENT ISOTROPIC DISPLACEMENT PARAMETERS FOR SAAMITE

Atom	Anion specification	Site occ. (%)	*x*	*y*	*z*	U_{eq} (Å^2)*
M^H(1)		100	0.1981(6)	0.3080(5)	0.3700(5)	0.0141(15)
M^H(2)		100	0.7906(5)	0.2659(4)	0.09441(12)	0.0079(9)
M^O(1)		100	0.5074(6)	0.7857(4)	0.22492(16)	0.0204(12)
M^O(2)		81	0.4967(14)	0.2873(12)	0.2303(4)	0.022(3)
M^O(3)		100	–0.0011(8)	0.0298(7)	0.2302(2)	0.0208(16)
M^O(4)		100	–0.0017(8)	0.5431(7)	0.2303(2)	0.0211(16)
Si(1)		100	0.6908(9)	0.0189(7)	0.3555(2)	0.0190(11)
Si(2)		100	0.6913(9)	0.5935(7)	0.3555(2)	0.0192(11)
Si(3)		100	0.2937(7)	0.9828(5)	0.10040(19)	0.0077(9)
Si(4)		100	0.2931(7)	0.5519(6)	0.10030(19)	0.0085(9)
A^P(1)		94	0.7617(2)	0.75515(15)	0.03112(5)	0.0090(4)
A^P(2)		26	0.209(3)	0.819(2)	0.3906(7)	0.021(3)
O(1)		100	0.660(2)	–0.0024(16)	0.2805(5)	0.016(2)
O(2)		100	0.458(3)	0.119(2)	0.3843(8)	0.035(3)
O(3)		100	0.707(3)	0.8080(19)	0.3852(6)	0.030(3)
O(4)		100	0.953(3)	0.120(2)	0.3824(7)	0.037(4)
O(5)		100	0.659(2)	0.5913(17)	0.2810(6)	0.017(2)
O(6)		100	0.459(3)	0.500(2)	0.3831(8)	0.041(4)
O(7)		100	0.953(3)	0.503(2)	0.3812(8)	0.040(4)
O(8)		100	0.322(2)	0.9835(16)	0.1745(5)	0.014(2)
O(9)		100	0.5277(19)	0.0732(14)	0.0715(5)	0.011(2)
O(10)		100	0.0359(19)	0.0737(15)	0.0717(5)	0.011(2)
O(11)		100	0.279(2)	0.7623(15)	0.0705(5)	0.012(2)
O(12)		100	0.324(2)	0.5718(16)	0.1747(5)	0.016(2)
O(13)		100	0.0350(19)	0.4513(15)	0.0717(5)	0.010(2)
O(14)		100	0.5248(19)	0.4457(15)	0.0717(5)	0.010(2)
X^O_M(1)	O	100	0.167(2)	0.291(2)	0.2871(6)	0.031(3)
X^O_M(2)	O	100	0.829(2)	0.2789(17)	0.1730(6)	0.018(2)
X^O_A(1)	(OH, F)	100	0.762(2)	0.7783(17)	0.1754(6)	0.021(3)
X^O_A(2)	(OH, F)	100	0.215(2)	0.790(2)	0.2783(6)	0.025(3)
X^P_M	H_2O	100	0.238(4)	0.330(3)	0.4792(9)	0.056(5)
X^P_A	(H_2O, □)	75	0.249(5)	0.742(4)	0.4956(12)	0.053(6)
W	(□, H_2O)	25	0.25(3)	0.86(3)	0.432(9)	0.05
Subsidiary peaks						
1		10	0.621(6)	0.626(4)	0.1999(14)	0.014(10)
2		3	0.653(6)	0.133(5)	0.2609(16)	0.02
3		2	0.260(9)	0.622(7)	0.532(2)	0.02
4		2	0.263(13)	0.081(10)	0.039(3)	0.02
5		5	0.219(7)	0.323(5)	0.391(4)	0.02
6		4	0.222(8)	0.799(6)	0.430(2)	0.02

*U_{iso} for A^P(2), O(10), O(14), X^P_A, W(fixed) and subsidiary peaks, fixed for subsidiary peaks 2–6.

$2M^{\mathbf{H}}$ and $1M^O$ sites are occupied by 2.09 Ti + 0.76 Nb + 0.13 Mn + 0.01 Mg + 0.01 Al (80.64 *epfu*), and the total refined scattering power at these sites (73.7 *epfu*, Table 9) reasonably agrees with the above composition. The refined site-scattering value at the M^H(1) site is significantly higher, 29.5 *epfu*, than that at the M^O(1) and M^H(2) sites, <22.1> *epfu*, indicating that the heavier atoms, particularly Nb, must be assigned to the M^H(1) site. In accordance with our knowledge (see above), we assign Mn [r = 0.83 Å, Shannon (1976)] to the M^O(1) site in the O sheet: 0.77 Ti + 0.13 Mn + 0.09 Nb + 0.01 Mg. We assign Ti, less Nb, and minor Al to the [5]-coordinated M^H(2) site. There is a good match between observed and calculated mean bond-lengths for all three sites, M^H(1,2) and M^O(1) (Table 9).

Consider next the alkali-cation sites in the O sheet, M^O(2)–M^O(4). Table 4 gives 2.22 Na + 0.55 Mn +

TABLE 8. SELECTED INTERATOMIC DISTANCES (Å) AND ANGLES (°) FOR SAAMITE

$M^O(1)$–$X^O_A(1)$	1.84(1)	$M^O(2)$–$X^O_M(1)$	2.28(1)	$M^O(3)$–O(8)b	2.25(1)
$M^O(1)$–O(1)a	2.01(1)	$M^O(2)$–$X^O_M(2)$	2.30(1)	$M^O(3)$–O(10)c	2.25(1)
$M^O(1)$–O(5)	2.01(1)	$M^O(2)$–O(5)	2.50(1)	$M^O(3)$–$X^O_A(2)$b	2.31(1)
$M^O(1)$–O(12)	2.03(1)	$M^O(2)$–O(1)	2.51(1)	$M^O(3)$–$X^O_M(1)$	2.32(2)
$M^O(1)$–O(8)	2.03(1)	$M^O(2)$–O(12)	2.55(1)	$M^O(3)$–$X^O_M(2)$c	2.36(1)
$M^O(1)$– $X^O_A(2)$	2.06(1)	$M^O(2)$–O(8)b	2.56(1)	$M^O(3)$–$X^O_A(1)$d	2.40(1)
$\langle M^O(1)–\varphi\rangle$	2.00	$\langle M^O(2)–O\rangle$	2.45	$\langle M^O(3)–\varphi\rangle$	2.32
$M^O(4)$–O(12)	2.26(1)	Si(1)–O(1)	1.62(1)	Si(2)–O(5)	1.61(1)
$M^O(4)$–O(5)c	2.26(1)	Si(1)–O(2)	1.62(2)	Si(2)–O(6)	1.61(2)
$M^O(4)$–$X^O_A(2)$	2.27(1)	Si(1)–O(4)	1.64(2)	Si(2)–O(7)	1.62(2)
$M^O(4)$–$X^O_M(2)$c	2.34(1)	Si(1)–O(3)b	1.68(1)	Si(2)–O(3)	1.63(1)
$M^O(4)$–$X^O_M(1)$	2.36(1)	$\langle$Si(1)–O$\rangle$	1.64	$\langle$Si(2)–O$\rangle$	1.62
$M^O(4)$–$X^O_A(1)$c	2.40(1)				
$\langle M^O(1)–\varphi\rangle$	2.32	Si(3)–O(8)	1.60(1)	Si(4)–O(12)	1.60(1)
		Si(3)–O(10)2	1.62(1)	Si(4)–O(13)	1.63(1)
Si(1)a–O(3)–Si(2)	134.3(9)	Si(3)–O(9)2	1.62(1)	Si(4)–O(14)	1.63(1)
Si(3)–O(11)–Si(4)	134.6(7)	Si(3)–O(11)	1.67(1)	Si(4)–O(11)	1.67(1)
$\langle$Si–O–Si$\rangle$	134.5	$\langle$Si(3)–O$\rangle$	1.63	$\langle$Si(4)–O$\rangle$	1.63
$M^H(1)$–$X^O_M(1)$	1.78(2)	$M^H(2)$–$X^O_M(2)$	1.69(1)		
$M^H(1)$–O(4)c	1.94(1)	$M^H(2)$–O(14)	1.97(1)		
$M^H(1)$–O(7)c	1.95(2)	$M^H(2)$–O(9)	1.99(1)		
$M^H(1)$–O(6)	1.96(2)	$M^H(2)$–O(13)e	1.99(1)		
$M^H(1)$–O(2)	1.97(2)	$M^H(2)$–O(10)e	1.99(1)		
$M^H(1)$–X^P_M	2.35(2)	$\langle M^H(2)–O\rangle$	1.93		
$\langle M^H(1)–\varphi\rangle$	1.99				
$A^P(1)$–O(9)a	2.75(1)	$A^P(2)$–X^P_A	2.34(3)		
$A^P(1)$–O(13)e	2.76(1)	$A^P(2)$– $X^O_A(2)$	2.44(2)		
$A^P(1)$–O(10)f	2.78(1)	$A^P(2)$–O(7)c	2.58(2)		
$A^P(1)$–O(14)	2.79(1)	$A^P(2)$–O(6)	2.60(2)		
$A^P(1)$–O(11)	2.84(1)	$A^P(2)$–O(2)a	2.61(2)		
$A^P(1)$–O(11)e	2.85(1)	$A^P(2)$–O(4)h	2.62(2)		
$A^P(1)$–O(14)g	2.90(1)	$A^P(2)$–O(3)c	2.72(2)		
$A^P(1)$–O(10)g	2.91(1)	$A^P(2)$–O(3)	2.72(2)		
$A^P(1)$–O(9)g	2.91(1)	$\langle A^P(2)–\varphi\rangle$	2.58		
$A^P(1)$–O(13)g	2.92(1)				
$\langle A^P(1)–O\rangle$	2.84				

φ = unspecified anion;
a = x, y + 1, z; b = x, y – 1, z; c = x – 1, y, z; d = x – 1, y – 1, z; e = x + 1, y, z; f = x + 1, y + 1, z;
g = –x + 1, –y + 1, –z; h = x – 1, y + 1, z.

0.04 Fe^{2+} = 3 *apfu* with a total scattering of 39.21 *epfu*. Site scattering at the alkali sites varies from 8.6 to 15.3 *epfu* and the total scattering equals 38.80 *epfu*. Hence Na must be the dominant cation species at the M^O(2–4) sites. The M^O(2) site has a mean bond-length of 2.45 Å, whereas the M^O(3,4) sites have significantly shorter equal mean bond-lengths, 2.32 Å, indicating that the larger Na (r = 1.02 Å) must be assigned to the M^O(2) site, whereas the cations smaller than Na, namely Mn (r = 0.83 Å) and Fe^{2+} (r = 0.78 Å), can be assigned to the M^O(3,4) sites. This assignment is supported by individual site-scattering values. As the M^O(3) and M^O(4) sites have site-scattering values of 14.9 and 15.3 *epfu*, respectively, we assign more Mn to the M^O(4) site (Table 9). The occurrence of both Na and Mn at one site is fairly common in Group-III TS-block minerals; it has been previously described for vuonnemite (Ercit *et al.* 1998), bornemanite (Cámara & Sokolova 2007), nechelyustovite (Cámara & Sokolova 2009), and kazanskyite (Cámara *et al.* 2012). We assign the remaining Na to the M^O(2) site: 0.81 Na + 0.19 □ (Table 9).

Let us consider lastly the peripheral A^P(1,2) sites, with refined site-scattering values of 45.3 and 5.2 *epfu*, respectively (Table 9). The cations to be assigned to these sites are Ba, Sr, K, and Ca, with a total scattering 49.43 *epfu* (Table 4). Atoms at the A^P(1) site form a layer with a topology (see text below) that is similar to the cation layer in several Group-III TS-block structures: barytolamprophyllite (Sokolova & Cámara 2008), bornemanite

TABLE 9. REFINED SITE-SCATTERING AND ASSIGNED SITE-POPULATIONS FOR SAAMITE

Site**	Refined site-scattering (*epfu*)	Assigned site-population (*apfu*)	Calculated site-scattering (*epfu*)	<X-φ>$_{calc.}$* (Å)	<X-φ>$_{obs.}$ (Å)	Ideal composition (*apfu*)
		Cations				
M^H(1)	29.5(1.5)	0.55 Nb + 0.45 Ti	32.45	2.00	1.99	Nb
[5]M^H(2)	22.5(4)	0.87 Ti + 0.12 Nb + 0.01 Al	24.19	1.90	1.93	Ti
M^O(1)	21.7(4)	0.77 Ti + 0.13 Mn + 0.09 Nb + 0.01 Mg	24.00	2.01	2.00	Ti
M^O(2)	8.6(4)	0.81 Na + 0.19 □	8.91	2.40	2.45	Na
M^O(3)	14.9(4)	0.72 Na + 0.26 Mn + 0.02 Fe^{2+}	14.94	2.35	2.32	Na
M^O(4)	15.3(4)	0.69 Na + 0.29 Mn + 0.02 Fe^{2+}	15.36	2.33	2.32	Na
[10]A^P(1)	45.3(5)	0.61 Ba + 0.20 Sr + 0.13 K + 0.06 □	44.23	2.88	2.84	Ba
[8]A^P(2)	5.2***	0.26 Ca + 0.74 □	5.2	2.49	2.58	□
		Anions				
[3]X^O_A(1)		0.63 OH + 0.37 F				OH
X^O_A(2)		0.63 OH + 0.37 F				OH
[1]X^P_M		1.00 H_2O				H_2O
[1]X^P_A		0.75 H_2O + 0.25 □				H_2O
W		0.25 H_2O + 0.75 □				□

X = cation, φ = O, OH, F, H_2O;
*calculated by summing constituent ionic radii; values from Shannon (1976);
**coordination number is given only for non-[6]-coordinated sites;
***site scattering was refined and then fixed at the last stages of the refinement (see discussion in text).

(Cámara & Sokolova 2007), nechelyustovite (Cámara & Sokolova 2009), and kazanskyite (Cámara *et al.* 2012) (Table 1). In accordance with our knowledge of the composition of the A^P site in the structures listed above, we assign Ba, Sr, and K to the A^P(1) site, and there is a good agreement between the refined and calculated values of the site scattering: 45.3 and 44.23 *epfu*, respectively (Table 9). In accordance with the refined site-scattering of 5.2 *epfu*, we assign available 0.26 Ca *apfu* to the A^P(2) site. Therefore at the A^P(1) and A^P(2) sites, Ba and vacancy, respectively, are the dominant species (Table 9).

Description of the structure

Site nomenclature. As stated above, the cation sites are divided into three groups: M^O sites of the O sheet, M^H and *Si* sites of the H sheet, and peripheral A^P sites. Also in accordance with Sokolova (2006), we label the X anions as follows: X^O = anions of the O sheet not coordinating SiO_4 tetrahedra of Si_2O_7 groups; X^O_M = anion at the common vertex of four polyhedra, 3 M^O and M^H; X^O_A = anion at the common vertex of four polyhedra, 3 M^O and A^P, where A^P–$X^O_A \leq 3$ Å or at the common vertex of three M^O octahedra where A^P–$X^O_A > 3$ Å, and hence the X^O_A anion does not coordinate the A^P atom; X^P = X^P_M and X^P_A = apical anions of M^H and A^P at the periphery of the TS block.

Cation sites. In the crystal structure of saamite, there is one TS block composed of H_1OH_2 sheets.

There are four cation sites in the O sheet: the Ti-dominant M^O(1) site and the alkali-cation M^O(2–4) sites (Fig. 3a). The M^O(1) site is occupied mainly by Ti and is coordinated by four O atoms and two monovalent X^O_A anions (see section on *Anion sites* below) with a <M^O(1)–φ> distance of 2.00 Å (φ = unspecified anion) (Tables 7, 8, 9). The M^O(2) site is occupied by Na at 81% (Table 9) and is coordinated by six O atoms, with a <M^O(2)–O> distance of 2.45 Å. The M^O(3) and M^O(4) sites are occupied by Na at ~70% and M^{2+} (= Mn and Fe^{2+}) at ~30% (Table 9); they are coordinated by four O atoms and two X^O_A anions, with <M^O(3)–φ> = <M^O(4)–φ> = 2.32 Å. For the O sheet, the total of the 4M^O cations is $[(Na_{2.22}Mn_{0.55}\ Fe^{2+}_{0.04}\square_{0.19})(Ti_{0.77}\ Mn_{0.13}Nb_{0.09}Mg_{0.01})]_{\Sigma 4}$, with simplified and ideal compositions $(Na,Mn)_3Ti$ and Na_3Ti *apfu*, respectively.

In the H_1 and H_2 sheets, there are four tetrahedrally coordinated sites occupied by Si, with a grand <<Si–O>> distance of 1.63 Å (Table 8, Figs. 3b, 3c). There are two M^H sites that occur in different H sheets of the TS block. In the H_1 sheet (Fig. 3b), the [5]-coordinated M^H(2) site is occupied mainly by Ti (Table 9) and is coordinated by five O atoms, with a <M^H(2)–O> distance of 1.93 Å; the very short M^H(2)–X^O_M(2) distance of 1.69 Å (Table 8) is in accordance with the structure topology of Group-III

TABLE 10. BOND-VALENCE VALUES* FOR SAAMITE

Atom	Si(1)	Si(2)	Si(3)	Si(4)	$M^{O}(1)$	$M^{O}(2)$	$M^{O}(3)$	$M^{O}(4)$	$M^{H}(1)$	$M^{H}(2)$	$A^{P}(1)$	$A^{P}(2)$	Σ
O(1)	1.01				0.59	0.13	0.26						1.99
[3]O(2)	1.01								0.76			0.05	1.82
O(3)	0.86	0.97										0.04	1.91
												0.04	
[3]O(4)	0.95								0.81			0.05	1.81
O(5)		1.03			0.59	0.13		0.25					2.00
[3]O(6)		1.03							0.77			0.05	1.85
[3]O(7)		1.01							0.79			0.05	1.85
O(8)			1.06		0.57	0.12	0.26						2.01
O(9)			1.01							0.64	0.23		2.03
											0.15		
O(10)			1.01							0.64	0.21		2.01
											0.15		
O(11)			0.88	0.88							0.19		2.13
											0.18		
O(12)				1.06	0.57	0.12		0.25					2.00
O(13)				0.97						0.64	0.22		1.97
											0.14		
O(14)				0.97						0.66	0.21		2.00
											0.16		
$X^{O}_{M}(1)$						0.19	0.22	0.21	1.27				1.89
$X^{O}_{M}(2)$						0.18	0.21	0.22		1.47			2.08
[3]$X^{O}_{A}(1)$					0.88		0.18	0.17					1.23
$X^{O}_{A}(2)$					0.46		0.21	0.23				0.07	0.97
[1]X^{P}_{M}									0.30				0.30
[1]X^{P}_{A}												0.08	0.08
Total	3.83	4.04	3.96	3.88	3.66	0.87	1.34	1.33	4.70	4.05	1.84	0.43	
Aggregate charge	4.00	4.00	4.00	4.00	3.81	0.81	1.28	1.31	4.55	4.11	1.75	0.52	

*bond-valence parameters (*vu*) are from Brown (1981); coordination numbers are shown for non-[4]-coordinated anions; bond-valence parameters cation-F and cation-O were used for $X^{O}_{A}(1,2)$ anions of the composition $(O_{0.63}F_{0.37})$.

minerals (Sokolova 2006, Fig. 31). In the H_2 sheet (Fig. 3c), the [6]-coordinated Nb-dominant $M^{H}(1)$ site is coordinated by five O atoms and an H_2O group with a $\langle M^{H}(1)–\varphi\rangle$ distance of 1.99 Å (Table 8). The H_2O group is the X^{P}_{M} anion following Sokolova (2006). The shortest $M^{H}(1)–X^{O}_{M}(1)$ distance is 1.78 Å and the longest $M^{H}(1)–X^{P}_{M}$ distance is 2.35 Å, from the $M^{H}(1)$ atom to an H_2O group. For the H_1 and H_2 sheets, the total of $(M^{H})_2$ cations is $[(Ti_{0.87}Nb_{0.12}Al_{0.01})(Nb_{0.55}Ti_{0.45})]_{\Sigma 2}$, with simplified and ideal compositions Ti(Nb,Ti) and TiNb *apfu*, respectively.

In saamite, there are two A^{P} sites. The [10]-coordinated $A^{P}(1)$ site is occupied by $Ba_{0.61}Sr_{0.20}K_{0.13}\square_{0.06}$ *pfu* and is coordinated by O atoms, with $\langle A^{P}(1)–O\rangle$ = 2.84 Å. The [8]-coordinated $A^{P}(2)$ site is occupied by $\square_{0.74}Ca_{0.26}$ *pfu* (Table 9) and is coordinated by six O atoms, one monovalent anion $X^{O}_{A}(2)$ and one H_2O group, namely an X^{P}_{A} anion in the terminology of Sokolova (2006), with $\langle A^{P}(2)–\varphi\rangle$ = 2.58 Å. At the $A^{P}(1)$ and $A^{P}(2)$ sites, the dominant species are Ba and □, respectively, and we write the ideal composition of these sites as Ba *apfu* and □ *pfu* (Table 9). To summarize, simplified and ideal compositions of two peripheral sites are Ba(□,Ca) and Ba□ *pfu*, respectively.

We can write the cation part of the ideal structural formula as the sum of (1) the peripheral sites + (2) two H sheets + (3) O sheet, namely: (1) Ba□ + (2) TiNb + (3) Na_3Ti = Ba□TiNbNa_3Ti, with a total charge of 18^{+}.

Anion sites. There are 14 anion sites, O(1–14), occupied by O atoms which form the tetrahedral coordination of the Si atoms (Tables 7, 8, 10). There are two anions, $X^{O}_{M}(1,2)$, each coordinating one M^{H} and three M^{O} atoms of the O sheet (Table 7). These anions receive bond valences of 1.89 and 2.08 *vu*, respectively (Table 10), and hence they are O atoms (Table 7). The $X^{O}_{A}(1)$ anion coordinates three M^{O} atoms: $M^{O}(1)$ (Ti), $M^{O}(3)$ (Na,Mn), and $M^{O}(4)$ (Na, Mn). The $X^{O}_{A}(2)$ anion coordinates three M^{O} atoms,

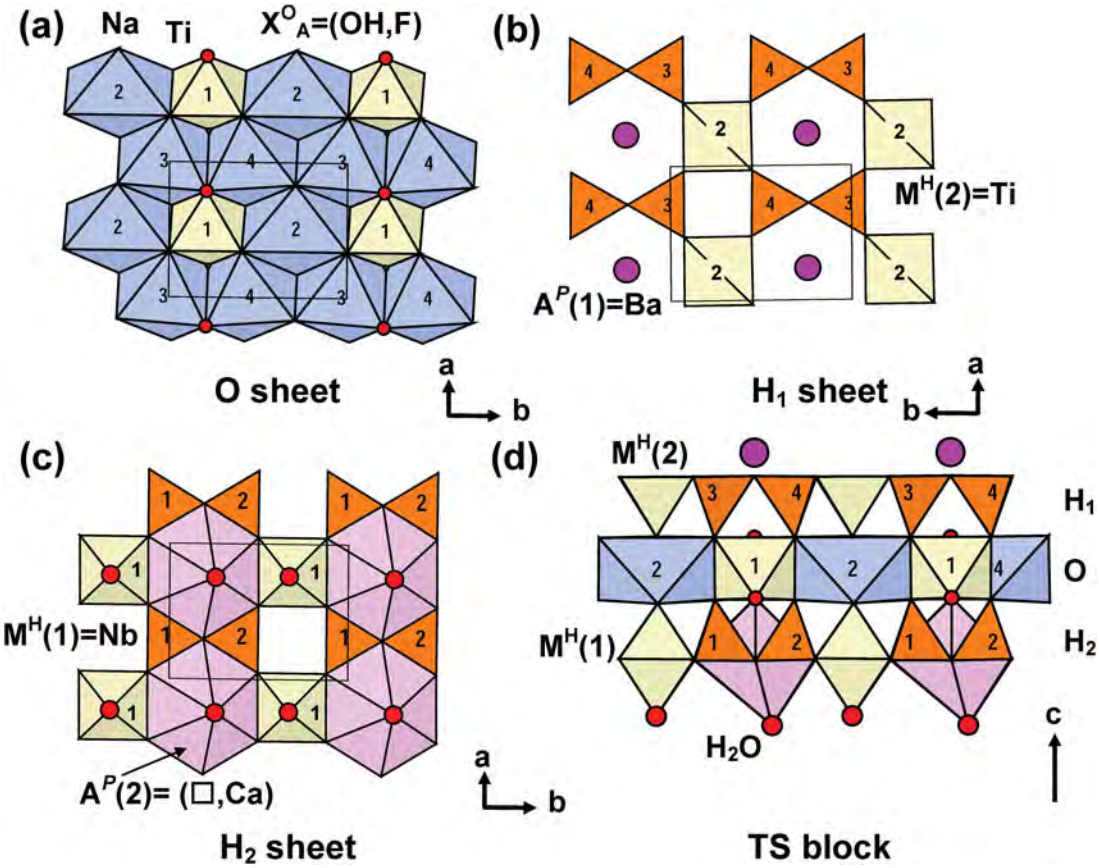

FIG. 3. The details of the TS block in the crystal structure of saamite: the close-packed octahedral (O) sheet (a); the heteropolyhedral (H) sheets H_1 (b) and H_2 (c); the TS block (d) viewed down [100]; SiO_4 tetrahedra are orange, Ti- and Nb-dominant polyhedra are yellow, Na-dominant octahedra are blue, and Ca-dominant $A^P(2)$-polyhedra are pink. $A^P(1)$ atoms are shown as large raspberry spheres, whereas monovalent X^O_A anions and H_2O groups are shown as small and medium red spheres, respectively. In (a) and (d), labels 1–4 correspond to $M^O(1–4)$, respectively. In (b) and (c), labels 1–4 (on orange) correspond to Si(1–4) tetrahedra, and labels 1 and 2 (on yellow) correspond to $M^H(1)$ and $M^H(2)$ polyhedra, respectively.

$M^O(1)$ (Ti), $M^O(3)$ (Na,Mn), $M^O(4)$ (Na,Mn), and the $A^P(2)$ (Ca) atom. They receive bond valences of 1.32 and 0.97 *vu*, respectively (Table 10), and hence are monovalent anions (Table 7). Because the chemical analysis gives F 0.74 *apfu,* we would need 2 – 0.74 = 1.26 OH *pfu* to fill these two sites (Tables 4, 9). Therefore, we could assign $OH_{0.63}F_{0.37}$ to each of the two $X^O_A(1,2)$ sites. Ideally, the two X^O_A sites give $(OH)_2$ *pfu*. Regarding the two X^P anions, X^P_M is an apical anion for the $M^H(1)$ cation (Table 8) and it receives a bond valence of 0.30 *vu* (Table 10); therefore it can be considered an H_2O group. The X^P_A anion coordinates the Ca atom when the $A^P(2)$ site is occupied by Ca at 26% (Tables 8, 9); it receives bond valence of 0.08 *vu* (Table 10) and can be considered an H_2O group. There is a coupled disorder of the Ca atoms at the $A^P(2)$ site and H_2O groups at the X^P_A and *W* sites separated by short distances $A^P(2)$–W = 0.96(19) Å and X^P_A–W = 1.67(19) Å. In agreement with the refined site-occupancies for the X^P_A and *W* sites, we assign $[(H_2O)_{0.75}\square_{0.25}]$ and $[\square_{0.75}(H_2O)_{0.25}]$ *pfu* to the X^P_A and *W* sites. Hence these two sites give just one H_2O *pfu*. Details of the short-range-order arrangements involving Ca atoms at the $A^P(2)$ site and H_2O groups at the X^P_A and *W* sites will be discussed below.

Summarizing, we can write the anion part of the ideal structural formula as the sum of the anions at specific sites: O_{14} (O atoms of Si_4 tetrahedra) + $O_2[X^O_M(1,2)]$+ $(OH)_2[X^O_A(1,2)]$+$(H_2O)_2[X^P_M$+$(X^P_A$+W)]. We consider an Si_2O_7 group as a complex oxyanion and therefore

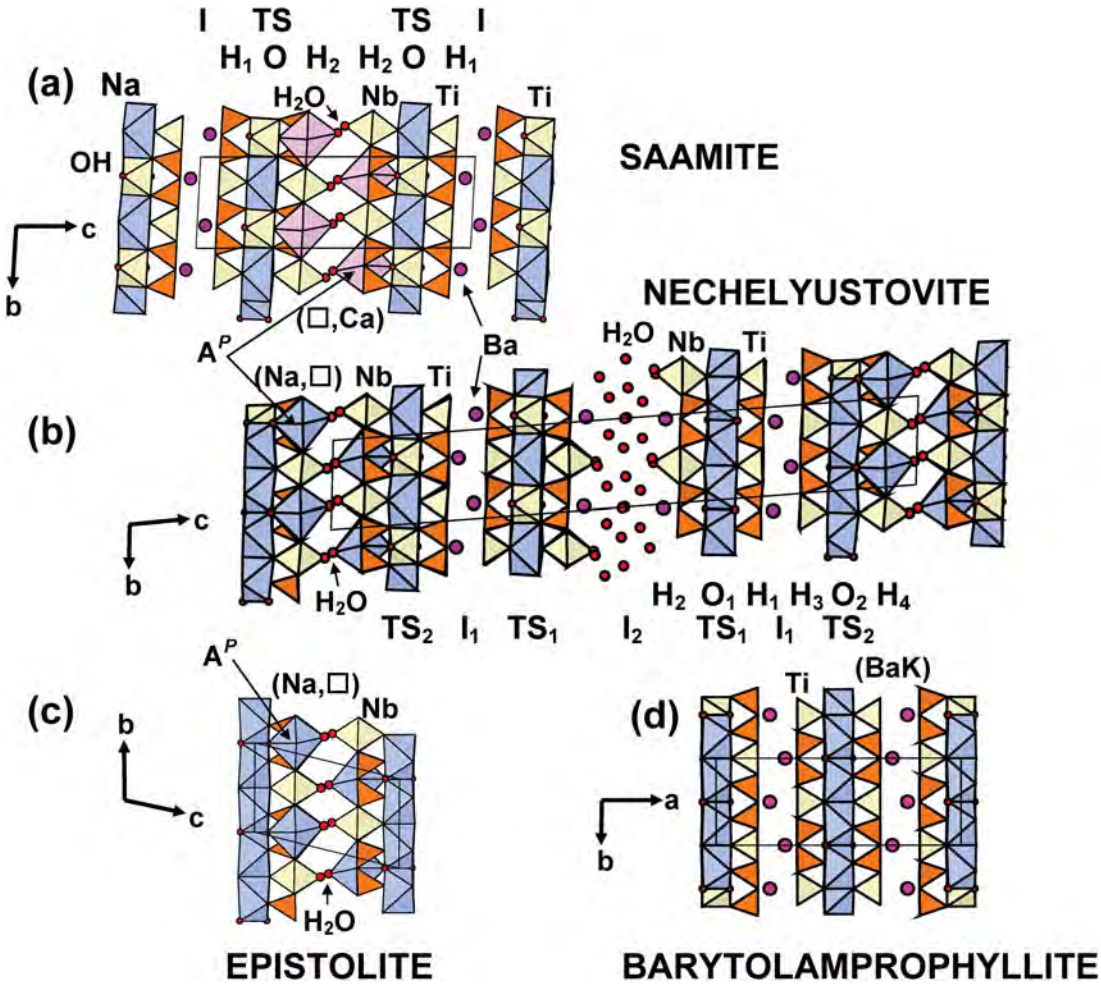

FIG. 4. The crystal structures of: saamite (a), nechelyustovite (b), and epistolite (c) projected onto (100), and barytolamprophyllite (d) projected onto (010). Legend as in Figure 3, Ca-dominant polyhedra are pink, (BaK) atoms are shown as large raspberry spheres. For saamite and nechelyustovite, TS and **I** blocks and H and O sheets are labeled.

write the anion part of the ideal structural formula as $(Si_2O_7)_2O_2(OH)_2(H_2O)_2$ with a total charge of 18^-.

We write the ideal structural formula of saamite as the sum of the cation and anion components: $Ba\square TiNbNa_3Ti(Si_2O_7)_2O_2(OH)_2(H_2O)_2$, space group $P\bar{1}$, $Z = 2$. The validity of the ideal formula is supported by the good agreement between the total charges for cations in the ideal and empirical formulae: 5^+ [for $Ba\square Na_3$] + 13^+ [Ti_2Nb] = 18^+ *versus* 5.67^+ [$(Ba_{0.61}Ca_{0.26}Sr_{0.20}K_{0.13})$ + $(Na_{2.22}Mn_{0.55}Fe^{2+}_{0.04})$] + 12.47^+ [$Ti_{2.09}Nb_{0.76}Mn_{0.13}Mg_{0.01}Al_{0.01}$] = 18.14^+.

Structure topology

The main structural unit in the crystal structure of saamite is the TS (Titanium Silicate) block (Sokolova 2006), which consists of HOH sheets, where H is a heteropolyhedral sheet including Si_2O_7 groups, and O is a trioctahedral close-packed sheet. In saamite, there is one unique TS block which consists of H_1OH_2 sheets (Fig. 3). The O sheet comprises $M^O(1–4)$ octahedra (Fig. 3a). There are two distinct H sheets in saamite. In the H_1 sheet, Si_2O_7 groups share common vertices with [5]-coordinated Ti-dominant $M^H(2)$ polyhedra (Fig. 3b). In the H_2 sheet, Si_2O_7 groups share common vertices with Nb-dominant $M^H(1)$ octahedra (Fig. 3c). The topology of the two H sheets is identical except for the coordination of the M^H atoms. In the H_1 and H_2 sheets, the peripheral sites are occupied by [10]-coordinated Ba [$A^P(1)$] and [8]-coordinated (□,Ca) [$A^P(2)$]. The H and O sheets link *via* common vertices of M^H, Si, $A^P(2)$, and M^O polyhedra to form the TS

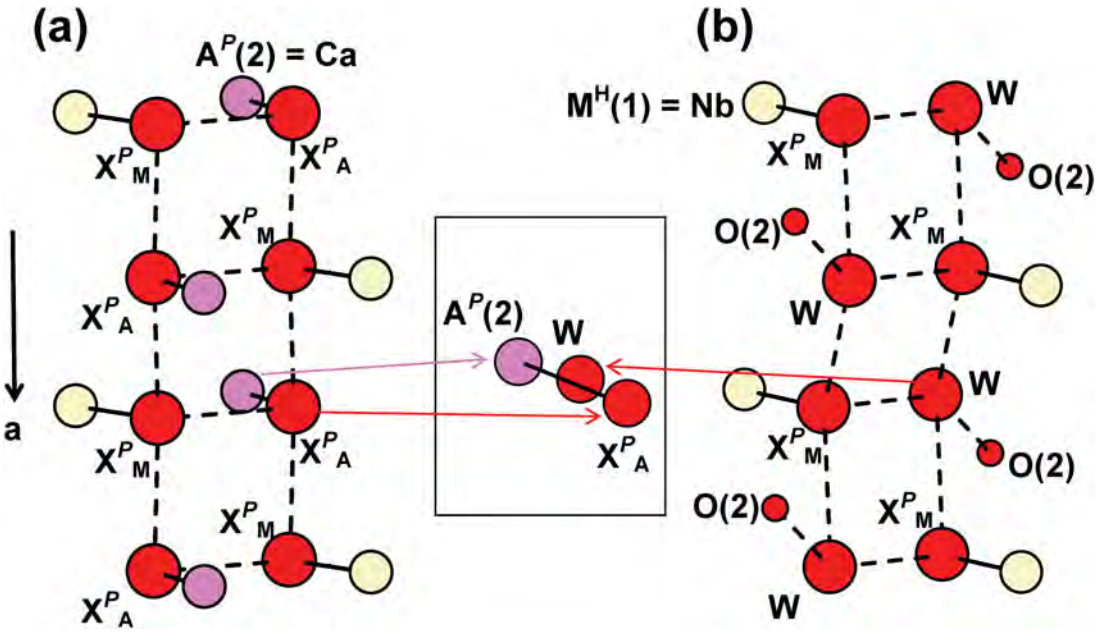

FIG. 5. Possible hydrogen bonding in the crystal structure of saamite for two short-range-order arrangements: SRO-1 (75%-occupancy) (a) and SRO-2 (25%-occupancy) (b). The inset shows positions of the $A^P(2)$ [= Ca] atoms and O atoms of H_2O groups at the *W* and X^P_A sites. O(2) and O atoms of H_2O groups, (X^P_M, X^P_A, and W), are shown as small and large red spheres, [8]-coordinated $A^P(2)$ [= Ca] and $M^H(1)$ [= Nb] atoms are shown as pink and yellow spheres, bonds $A^P(2)$–X^P_A and $M^H(2)$–X^P_M are shown as black solid lines and directions of possible hydrogen bonds are shown as dashed lines.

block which is parallel to (001) (Fig. 3d). In saamite, the TS block exhibits linkage 1 and a stereochemistry typical of Group III (Sokolova 2006): Si_2O_7 groups of the two H sheets link to the *trans* edges of the Ti octahedron of the O sheet.

In saamite, there are two types of self-linkage of TS blocks. The first type of self-linkage occurs between adjacent H_2 sheets of TS blocks (Fig. 4a). Here, two TS blocks connect through hydrogen bonding between H_2O groups [at X^P_M and X^P_A sites] which coordinate $M^H(1)$ [Nb] and $A^P(2)$ [Ca] cations as in the Group-III minerals nechelyustovite (Cámara & Sokolova 2009) (Fig. 4b) and epistolite (Sokolova & Hawthorne 2004) (Fig. 4c), and murmanite, a Group-IV mineral (Cámara *et al.* 2008) (see discussion below). This is type-[3] self-linkage of adjacent TS blocks (Sokolova 2006).

The second type of self-linkage occurs where the TS blocks alternate with intermediate (**I**) blocks: a layer of Ba atoms [$A^P(1)$ site] forms the **I** block between H_1 sheets of adjacent TS blocks (Fig. 4a), as in nechelyustovite (Fig. 4b) and barytolamprophyllite (Sokolova & Cámara 2008). This is type-[4] self-linkage of adjacent TS blocks, via additional cations in the **I** block (Sokolova 2006). In the **I** block, Ba atoms are arranged in a close-packed fashion where each atom is surrounded by six others at approximately equal distances of 5 Å. The composition of the **I** block is $[A^P(1)]_2$ or ideally Ba_2 (= Ba *apfu*).

To conclude, the crystal structure of saamite (Fig. 4a) consists of TS and **I** blocks alternating along **c**. There are two TS blocks and one **I** block per *c* cell-parameter. Furthermore, adjacent TS blocks connect through hydrogen bonding between H_2O groups. Saamite is the third TS-block mineral [after nechelyustovite and cámaraite, a Group-II mineral (Cámara *et al.* 2009)] with two different types of self-linkage of TS blocks: (1) through the **I** block with a layer of cations, and (2) via hydrogen bonding. The TS block exhibits the stereochemistry of Group III where Ti (+ Nb + Mg) equals 3 *apfu* (Sokolova & Cámara 2013), and this is the key to understanding the relationship between saamite and other TS-block minerals.

Hydrogen bonding and short-range order (SRO)

There is some cation and anion disorder in the epistolite-like part of the structure of saamite. The $A^P(2)$ site is 26% occupied by Ca; the X^P_A and *W* sites are partly (75 and 25%, respectively) occupied by H_2O (Table 9). There are short distances of 1.67 Å between the $A^P(2)$ site and the *W* site and 0.96 Å

between the X^P_A site and the *W* site; hence the *W* site can be occupied by H_2O where the associated $A^P(2)$ and X^P_A sites are vacant, *i.e.*, at 25% (and vice versa, at 75%). We consider two short-range-order (SRO) arrangements: (1) SRO-1 (75% occupancy) where H_2O groups occur at the X^P_A site, and either Ca atoms occur at the $A^P(2)$ site (26% occupancy), or the $A^P(2)$ site and the *W* site are vacant (Fig. 5a), and (2) SRO-2 (25% occupancy) where H_2O groups occur at the *W* site and the X^P_A and $A^P(2)$ sites are vacant. Table 11 reports O–O distances between O atoms of H_2O groups that occupy the X^P_M, X^P_A, and *W* sites for both arrangements. We modeled both SRO arrangements after the hydrogen-bonding arrangement in murmanite, ideally $Na_2Ti_2Na_2Ti_2(Si_2O_7)_2O_4(H_2O)_4$, where the stereochemistry of the hydrogen bonding has been established based on positions of H atoms of the H_2O groups (Cámara *et al*. 2008). Although murmanite is a Group-IV mineral and has a TS block of different topology and chemistry than that in epistolite, these two minerals have structures that consist exclusively of TS blocks and have the same type of self-linkage of TS blocks, *i.e.*, via hydrogen bonding between H_2O–H_2O groups and H_2O–O atoms of adjacent TS blocks. Hence we feel confident using the murmanite model of hydrogen bonding for the epistolite-like part of the saamite structure. Note that distances between O atoms at the X^P_M and *W* sites are 3.6 and 3.7 Å, too long for D (donor)–A(acceptor) distances (< 3.2 Å). We suggest that the position of the O atom of the H_2O group at the *W* site (occupied only at 25%) is not very accurate due to the character of the crystal used for the structure solution and refinement (R_1 value is rather high, 9.92%, as for other mineral structures found in the same sample).

The Ideal Structural Formula of Saamite

Above, we wrote simplified and ideal formulae of saamite based on the occupancies of the cation and anion sites. Here, we write the ideal structural formula of the TS block in saamite in accordance with Sokolova (2006): $A^P_2M^H_2M^O_4(Si_2O_7)_2X^O_4X^P_MX^P_A$, where A^P are cations at the peripheral (*P*) sites; M^H and M^O are cations of the H and O sheets; X^O are anions of the O sheet; X^P_M and X^P_A are apical anions of the M^H and A^P cations at the periphery of the TS block. In saamite, $A^P_2 = A^P(1) + A^P(2) = Ba + \square = Ba\square$; $M^H_2 = M^H(2) + M^H(1) = TiNb$; $M^O_4 = Na_3Ti$; $X^O_4 = O_2(OH)_2$; $X^P_M + X^P_A = H_2O + H_2O = (H_2O)_2$. Hence, we write the ideal composition of the TS block as follows:

$$^{A^P}[Ba\square]^{M^H}[TiNb]^{M^O}[Na_3Ti](Si_2O_7)_2{}^{X^O}[O_2(OH)_2]$$
$$^{X^P_M}[H_2O]^{X^P_A}[H_2O] = Ba\square TiNbNa_3Ti(Si_2O_7)_2O_2(OH)_2(H_2O)_2, Z = 2.$$

Note that there is H_2O at the *W* site occupied at 25%, ideally $\square$ *pfu*. As the X^P_A and *W* sites are 0.96 Å apart, we do not count the *W* site as an individual position in the ideal formula.

There is one **I** block in saamite. It comprises the $A^P(1)$ atoms, which have already been counted in the formula of the TS block. Hence the ideal structural formula for saamite is of the form $A^P_2M^H_2M^O_4(Si_2O_7)_2X^O_4X^P_MX^P_A$, which translates to $Ba\square TiNbNa_3Ti(Si_2O_7)_2O_2(OH)_2(H_2O)_2$, with $Z = 2$.

TABLE 11. POSSIBLE HYDROGEN BONDING IN SAAMITE

D···A	D···A (Å)
$X^P_M(H_2O)\cdots X^P_A(H_2O)a$	2.81(3)
$X^P_M(H_2O)\cdots X^P_A(H_2O)b$	2.84(3)
$X^P_M(H_2O)\cdots X^P_A(H_2O)$	2.94(3)
$X^P_M(H_2O)\cdots W(H_2O)b$	3.6(2)
$X^P_M(H_2O)\cdots W(H_2O)a$	3.7(2)
$W(H_2O)\cdots O(2)c$	2.5(2)

a: $-x$, $-y + 1$, $-z + 1$; b: $-x + 1$, $-y + 1$, $-z + 1$; c: x, $y + 1$, z.

Related Minerals

Sokolova & Cámara (2010, 2013) introduced the concept of basic and derivative structures. They defined a basic TS-block structure as having four characteristics: (1) there is only one type of TS block; (2) the two H sheets of the TS block are identical; (3) there is only one type of **I** block or it is absent; (4) there is only one type of self-linkage of TS blocks. They defined a derivative structure as having one or more of the following three characteristics: (1) there is more than one type of TS block; (2) there is more than one type of **I** block; (3) there is more than one type of self-linkage of TS blocks. Furthermore, a derivative structure is related to two or more basic structures of the same Group and hence can be built by adding basic structures via sharing the central O sheet of the TS blocks of adjacent structural fragments. Hence a derivative structure retains the stereochemistry and topology of the TS block characteristic for the Group.

Sokolova & Cámara (2013) labeled basic and derivative structures by the appropriate letter (B and D) and assigned a number to each structure type within each Group. In Group III, they identified four basic structure types, B1(GIII)-B4(GIII), and three derivative structures: bornemanite, D1 (GIII); kazanskyite, D2(GIII); and nechelyustovite, D3(GIII) (Table 1). Saamite is the fourth Group-III TS-block mineral that has a derivative structure, we

label it D4(GIII) (Table 1). The crystal structure of saamite (Fig. 4a) is a combination of two basic structures: barytolamprophyllite, B1(GIII) (Fig. 4d), and epistolite, B3(GIII) (Fig. 4c): D4(GIII) = B1 (GIII) + B3(GIII) (Table 1). In the saamite structure, the TS block exhibits linkage and stereochemistry typical for Group III [Ti (+ Nb + Mg) = 3 *apfu*]: Si_2O_7 groups of two H sheets link to the Ti octahedron in the O sheet.

Saamite is closely related to nechelyustovite (Fig. 4b). Both minerals contain one **I** block of the same topology and composition (Figs. 4a, 4b): an **I** block which is a layer of Ba atoms. The chemical compositions of both M^{H} and A^{P} sites of the TS blocks are identical in saamite and nechelyustovite. In saamite and nechelyustovite, two TS-blocks link directly (without an intermediate block) via hydrogen bonding between H_2O groups as in epistolite.

Sokolova & Cámara (2013) predicted eight derivative structures in Group III: D4(GIII)–D11(GIII), each being a combination of two basic structures of Group III. Sokolova & Cámara (2013) predicted the D5(GIII) structure as a combination of epistolite and barytolamprophyllite structural fragments. They derived its ideal structural formula, $\square_2Ba_2Ti_2Nb_2Na_6Ti_2(Si_2O_7)_4\ O_4(OH)_4(H_2O)_4$ ($Z = 1$), as the sum of the ideal structural formulae of barytolamprophyllite, $(BaK)Ti_2Na_3Ti(Si_2O_7)_2O_2(OH)_2$, and epistolite, $(Na\square)Nb_2Na_3Ti(Si_2O_7)_2O_2(OH)_2(H_2O)_4$, with the accompanying substitution: ${}^{P}K^{+}_{baryto} + {}^{P}Na^{+}_{epist} \leftrightarrow {}^{P}Ba^{+}_{D5(GIII)} + {}^{P}\square_{D5(GIII)}$. The D5(GIII) structure of Sokolova & Cámara (2013) is a perfect match with the crystal structure of saamite, both topologically and stereochemically. In this paper, we label the saamite structure as D4(GIII) because it is the fourth derivative structure in Group-III [it corresponds to the predicted D5(GIII) structure in Sokolova & Cámara (2013)]. The prediction of the saamite structure is the second correct prediction of a TS-block structure after prediction of the crystal structure of kolskyite, $(Ca\square)Na_2Ti_4(Si_2O_7)_2O_4(H_2O)_7$, a Group-IV TS-block mineral (Sokolova & Cámara 2010, 2013, Cámara *et al.* 2013).

Acknowledgements

We are very grateful to Renato and Adriana Pagano, Milan, Italy, who provided a sample of nechelyustovite from their mineral collection (Collezione Mineralogica, sample #10161c) where saamite was discovered. We thank Cristian Biagioni and Natale Perchiazzi and Associate Editor Henrik Friis for a careful revision. FCH was supported by a Canada Research Chair in Crystallography and Mineralogy, by Discovery and Major Installation grants from the Natural Sciences and Engineering Research Council of Canada, and by Innovation Grants from the Canada Foundation for Innovation. FC thanks Frank Hawthorne for supporting a visiting research period in Winnipeg in 2013.

References

Anthony, J.W., Bideaux, R.A., Bladh, K.W., & Nichols, M.C. (1995) *Handbook of Mineralogy. Silica, Silicates.* Mineral Data Publishing, Tucson, Arizona, United States, **2(1)**, 355.

Brown, I.D. (1981) The bond-valence method: an empirical approach to chemical structure and bonding. *In* Structure and Bonding in Crystals II (M. O'Keeffe & A. Navrotsky, eds.). Academic Press, New York, New York, United States (1–30).

Cámara, F. & Sokolova, E. (2007) From structure topology to chemical composition. VI. Titanium silicates: the crystal structure and crystal chemistry of bornemanite, a group-III Ti-disilicate mineral. *Mineralogical Magazine* **71**, 593–610.

Cámara, F. & Sokolova, E. (2009) From structure topology to chemical composition. X. Titanium silicates: the crystal structure and crystal chemistry of nechelyustovite, a group III Ti-disilicate mineral. *Mineralogical Magazine* **73**, 887–897.

Cámara, F., Sokolova, E., Hawthorne, F.C., & Abdu, Y. (2008) From structure topology to chemical composition. IX. Titanium silicates: revision of the crystal chemistry of lomonosovite and murmanite, Group-IV minerals. *Mineralogical Magazine* **72**, 1207–1228.

Cámara, F., Sokolova, E., & Nieto, F. (2009) Cámaraite, $Ba_3Na\ Ti_4(Fe^{2+},Mn)_8(Si_2O_7)_4O_4(OH,F)_7$. II. The crystal structure and crystal chemistry of a new group-II Ti-disilicate mineral. *Mineralogical Magazine* **73**, 855–870.

Cámara, F., Sokolova, E., & Hawthorne, F.C. (2012) Kazanskyite, $Ba\square TiNbNa_3Ti(Si_2O_7)_2O_2\ (OH)_2(H_2O)_4$, a Group-III Ti-disilicate mineral from the Khibiny alkaline massif, Kola Peninsula, Russia: description and crystal structure. *Mineralogical Magazine* **76**, 473–492.

Cámara, F., Sokolova, E., Abdu, Y.A., Hawthorne, F.C., & Khomyakov, A.P. (2013) Kolskyite, $(Ca\square)Na_2Ti_4(Si_2O_7)_2O_4(H_2O)_7$, a Group-IV Ti-disilicate mineral from the Khibiny alkaline massif, Kola Peninsula, Russia: description and crystal structure. *Canadian Mineralogist* **51**, 921–936.

Chukanov, N.V., Pekov, I.V., Rastsvetaeva, R.K., Aksenov, S.M., Zadov, A.E., Van, K.V., Blass, G., Schüller, W., & Ternes, B. (2012) Lileyite, $Ba_2(Na,Fe,Ca)_3MgTi_2(Si_2O_7)_2O_2F_2$, a new lamprophyllite-group mineral from the Eifel volcanic area, Germany. *European Journal of Mineralogy* **24**, 181–188.

Dudkin, O.B. (1959) On barium lamprophyllite. *Zapiski Vsesoyuznogo Mineralogicheskogo Obshchestva* **88(6)**, 713–715 (in Russian).

Ercit, T.S., Cooper, M.A., & Hawthorne, F.C. (1998) The crystal structure of vuonnemite, $Na_{11}Ti^{4+}Nb_2(Si_2O_7)_2(PO_4)_2$

O_3(F,OH), a phosphate-bearing sorosilicate of the lomonosovite group. *Canadian Mineralogist* **36**, 1311–1320.

Krivovichev, S.V., Armbruster, T., Yakovenchuk, V.N., Pakhomovsky, Ya.A., & Men'shikov, Yu.P. (2003) Crystal structures of lamprophyllite-2*M* and lamprophyllite-2*O* from the Lovozero alkaline massif, Kola peninsula, Russia. *European Journal of Mineralogy* **15**, 711–718.

Mandarino, J.A. (1979) The Gladstone-Dale relationship. Part III. Some general applications. *Canadian Mineralogist* **17**, 71–76.

Mandarino, J.A. (1981) The Gladstone-Dale relationship. Part IV. The compatibility concept and its application. *Canadian Mineralogist* **19**, 441–450.

Nèmeth, P., Khomyakov, A.P., Ferraris, G., & Menshikov, Yu.P. (2009) Nechelyustovite, a new heterophyllosilicate mineral, and new data on bykovaite: a comparative TEM study. *European Journal of Mineralogy* **21**, 251–260.

Pouchou, J.L. & Pichoir, F. (1985) 'PAP' φ(ρZ) procedure for improved quantitative microanalysis. *In* Microbeam Analysis (J.T. Armstrong, ed.). San Francisco Press, San Francisco, California, United States (104–106).

Rastsvetaeva, R.K. & Chukanov, N.V. (1999) Crystal structure of a new high-barium analogue of lamprophyllite with a primitive unit cell. *Doklady Chemistry* **368(4–6)**, 228–231.

Shannon, R.D. (1976) Revised effective ionic radii and systematic studies of interatomic distances in halides and chalcogenides. *Acta Crystallographica* **A32**, 751–767.

Sheldrick, G.M. (2004) CELL_NOW. University of Göttingen, Germany.

Sheldrick, G.M. (2008) A short history of SHELX. *Acta Crystallographica* **A64**, 112–122.

Sokolova, E. (2006) From structure topology to chemical composition. I. Structural hierarchy and stereochemistry in titanium disilicate minerals. *Canadian Mineralogist* **44**, 1273–1330.

Sokolova, E. & Cámara, F. (2007) From structure topology to chemical composition. II. Titanium silicates: revision of the crystal structure and chemical formula of delindeite. *Canadian Mineralogist* **45**, 1247–1261.

Sokolova, E. & Cámara, F. (2008) From structure topology to chemical composition. III. Titanium silicates: crystal chemistry of barytolamprophyllite. *Canadian Mineralogist* **46**, 403–412.

Sokolova, E. & Cámara, F. (2010) From chemical composition to structure topology in Ti silicates. 20th General Meeting of the International Mineralogical Association, Collected Abstracts, Budapest, Hungary. *Acta Mineralogica-Petrographica Abstract Series* **6**, 732.

Sokolova, E. & Cámara, F. (2013) From structure topology to chemical composition. XVI. New developments in the crystal chemistry and prediction of new structure topologies for titanium disilicate minerals with the TS block. *Canadian Mineralogist* **51**, 861–891.

Sokolova, E. & Hawthorne, F.C. (2004) The crystal chemistry of epistolite. *Canadian Mineralogist* **42**, 797–806.

Sokolova, E. & Hawthorne, F.C. (2008) From structure topology to chemical composition. IV. Titanium silicates: the orthorhombic polytype of nabalamprophyllite from Lovozero massif, Kola Peninsula, Russia. *Canadian Mineralogist* **46**, 1469–1477.

Sokolova, E., Cámara, F., & Hawthorne, F.C. (2011) From structure topology to chemical composition. XI. Titanium silicates: crystal structures of innelite-1*T* and innelite-2*M* from Inagli massif, Yakutia, Russia, and the crystal chemistry of innelite. *Mineralogical Magazine* **75**, 2495–2518.

Volkova, M.I. & Melentiev, B.N. (1939) Chemical composition of the Khibiny apatites. *Comptes rendus de l'académie des sciences de l'U.R.S.S.* **25**, 120–122.

Wilson, A.J.C. (ed.) (1992) *International Tables for Crystallography. Volume C: Mathematical, physical and chemical tables*. Kluwer Academic Publishers, Dordrecht, Netherlands.

Received May 18, 2014, revised manuscript accepted October 16, 2014.